NASA TM-86721

NASA Technical Memorandum 86721

Airborne Astronomy Program
Medium Altitude Missions Branch
Preprint Series 030

Far-Infrared Emission Lines of CO and OH in the Orion-KL Molecular Shock

Dan M. Watson, R. Genzel,
C.H. Townes, and
J.M.V. Storey

September 1985

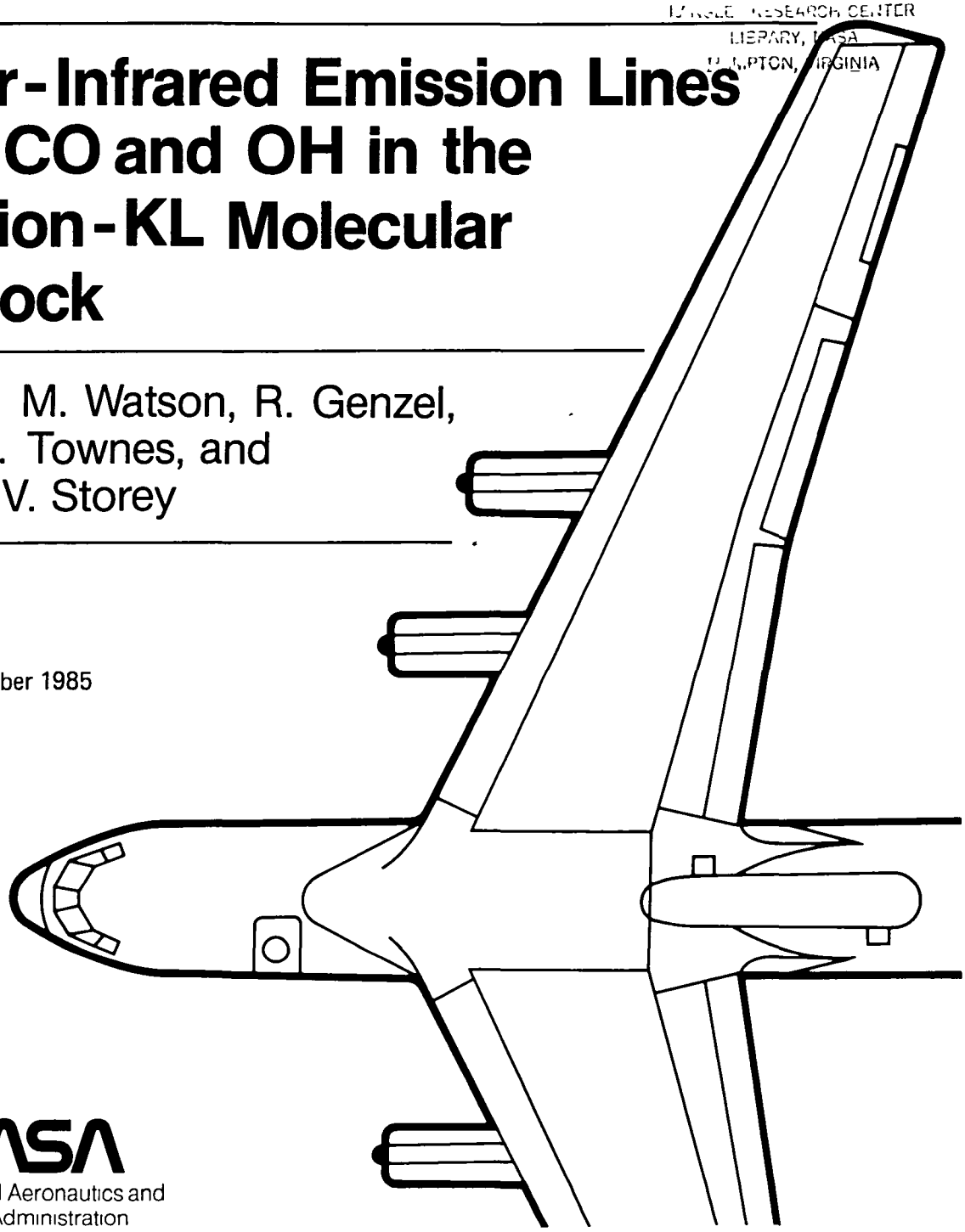

NASA
National Aeronautics and
Space Administration

NASA Technical Memorandum 86721

Airborne Astronomy Program
Medium Altitude Missions Branch
Preprint Series 030

Far-Infrared Emission Lines of CO and OH in the Orion-KL Molecular Shock

Dan M. Watson, University of California, Berkeley, California
California Institute of Technology, Pasadena, California
R. Genzel
C. H. Townes, University of California, Berkeley, California
J. M. V Storey, Anglo Australian Observatory, New South Wales, Australia
University of New South Wales, Kensington, Australia

September 1985

National Aeronautics and
Space Administration

Ames Research Center
Moffett Field, California 94035

FAR-INFRARED EMISSION LINES OF CO AND OH IN THE ORION-KL MOLECULAR SHOCK

Dan M. Watson[1,2], R. Genzel[1],

C. H. Townes[1] and J. W. V. Storey[3,4]

[1]Department of Physics, University of California, Berkeley
[2]Department of Physics, California Institute of Technology
[3]Anglo-Australian Observatory
[4]School of Physics, University of New South Wales

To appear in *The Astrophysical Journal*

ABSTRACT

Observations of far-infrared rotational emission lines which arise in the shocked gas associated with Orion-KL are presented, including detections of the CO $J = 34 \rightarrow 33$, $J = 31 \rightarrow 30$, $J = 26 \rightarrow 25$, and OH $^2\Pi_{3/2}\, J^p = 7/2^- \rightarrow 5/2^+$ emission lines, as well as improved measurements of the CO $J = 22 \rightarrow 21$ and OH $^2\Pi_{3/2}$ $J = 5/2 \rightarrow 3/2$ lines. These lines are observed to have velocity widths of $\Delta v \sim 20$-30 km s^{-1}, somewhat less than either the 2 μm H_2 lines or the high-velocity "plateau" component of the millimeter-wave CO lines seen in this object. An H_2 column density of $\sim 3 \times 10^{21}$ cm^{-2}, a total mass of ~ 1 $M_\odot$ and characteristic temperature and density $T \sim 750$ K and $n(H_2) \sim 2 \times 10^6$ cm^{-3} can be derived from the CO intensities. The density is too low by at least an order of magnitude for the observed infrared H_2 and far-infrared CO emission to be accounted for by a purely hydrodynamic shock, and support is lent to hydromagnetic shock models.

From the present measurements, the relative abundance of CO is estimated to be $CO/H_2 \approx 1.2 \times 10^{-4}$, corresponding to 20% of the cosmic abundance of C existing in the form of CO. The average relative abundance of OH in the shocked gas is $OH/H_2 \gtrsim 5 \times 10^{-7}$, more than an order of magnitude greater than that expected in the quiescent molecular material surrounding the shocked region. The CO lines are optically thin, and the OH lines have $\tau \gtrsim 3$. An upper limit to the intensity of the HD $J = 1 \rightarrow 0$ line is used to derive an upper limit of 4×10^{-5} for the D/H relative abundance in the Orion cloud core.

I. The Molecular Outflow in Orion-KL

Orion-KL, the molecular region associated with the Kleinmann-Low nebula, is the prototype of the class of "active" molecular cloud cores. This recently-recognized class is characterized by hypersonic mass outflow, affecting large portions of the cloud core, which is apparently driven by mass loss from a newly-formed star. The young star itself is generally manifested by a compact infrared source, and the outflow displays three main features: motions of compact objects, molecular lines involving states of very high excitation, and molecular lines with very large velocity widths. First noticed were the motions of H_2O masers (e.g. Knowles *et al.* 1969, Strelnitskii and Syunyaev 1973; Genzel and Downes 1977; Genzel *et al.* 1981) and of Herbig-Haro objects (e.g. Cudworth and Herbig 1979), which indicate large-scale expansion. Hot, shocked molecular matter associated with the outflows ($T \gtrsim 2000$ K) is seen in the near-infrared transitions of molecular hydrogen (e.g. Gautier *et al.* 1976; Beckwith *et al.* 1983). Molecular lines from these regions have widths as large as 100 km s^{-1} (e.g. Zuckerman, Kuiper and Rodriguez-Kuiper 1976; Nadeau, Geballe and Neugebauer 1982); the spatial distribution of different velocity components of these lines often indicates a bipolar morphology (e.g. Snell, Loren and Plambeck 1980; Bally and Lada 1983). Large amounts of energy and momentum may be fed into the surrounding molecular clouds during the lifetime of the outflow, and these objects might, therefore, play a role in the support of molecular clouds against self-gravity (cf. Bally and Lada 1983) and influence the rate of further star formation in these clouds.

To study the interactions between the outflow and more quiescent material, we examine the hot shocked gas that lies at their interface. The presently-available probes of this shocked gas include the rotation-vibration and pure rotational lines of H_2 in the near- and mid-infrared (cf. Beckwith *et al.* 1983, Beck 1984) and the far-infrared rotational lines of CO (Watson *et al.* 1980; Storey *et al.* 1981; Stacey *et al.*

1982, 1983) and OH (Storey, Watson and Townes 1981). The far-infrared lines of CO are of particular importance because they are density-sensitive, and thereby carry information on the shock's compression ratio.

In this paper we report observations of the far-infrared lines of CO and OH in the shocked matter associated with Orion-KL. The present data include the first detections of CO $J = 34 \rightarrow 33$ ($\lambda = 77.06$ μm), $J = 31 \rightarrow 30$ ($\lambda = 84.41$ μm), CO $J = 26 \rightarrow 25$ ($\lambda = 100.5$ μm), and OH $^2\Pi_{3/2}$ $J^p = 7/2^- \rightarrow 5/2^+$ ($\lambda = 84.60$ μm) lines, as well as improved measurements of the previously-observed lines CO $J = 22 \rightarrow 21$ ($\lambda = 118.6$ μm; Watson *et al.* 1980) and OH $^2\Pi_{3/2}$ $J = 5/2 \rightarrow 3/2$ ($\lambda = 119.2, 119.4$ μm; Storey, Watson and Townes 1981). The CO measurements and the parameters derived from them are consistent with our previous observations (Watson *et al.* 1980, Storey *et al.* 1981), but with the addition of the CO $J = 34 \rightarrow 33$ line provide stronger constraints on the density and compression ratio of the shock. The latter is shown to be too small for a simple, purely hydrodynamic shock to account for the observed activity. The data generally support the shock models of Chernoff, Hollenbach and McKee (1982) and Draine and Roberge (1982, 1984), in which magnetic effects are critically important to the shock's characteristics.

II. Observations

The instrument used in this experiment was the UC Berkeley tandem Fabry-Perot spectrometer (Storey, Watson and Townes 1980; Watson 1982). Observations were made using velocity resolutions of 60 km s^{-1} (at 77 and 84 μm), 75 km s^{-1} (at 100 and 112 μm), and 110 km s^{-1} (at 119 μm); the instrumental profile is a Lorentzian. The system noise equivalent power (NEP) was $1\text{-}2 \times 10^{-14}$ W Hz$^{-1/2}$, including all losses in the spectrometer, telescope and atmosphere. The observations took place in 1982 February and 1983 February on the 91.4 cm telescope of the NASA Kuiper Airborne Observatory. At the observing altitude of 12.5 km,

the water vapor column density along the line of sight was typically 20 microns. The system field of view was 44" in diameter (FWHM) and the solid angle of the beam was 5×10^{-8} sr for all observations except those at 84 μm, where the corresponding parameters were 30" and 2.7×10^{-8} sr. The telescope's oscillating secondary mirror was used to provide a 4' east-west chop at 29 Hz.

Each line was observed with the beam centered on the Becklin-Neugebauer object ($\alpha_{1950} = 5^h\ 32^m\ 46.^s7$, $\delta_{1950} = -5\ 24'\ 17''$). Additional points in a northwest-southeast strip were observed in the 119 μm OH lines. Line fluxes were derived from the measured line-to-continuum ratio and the photometric measurements of Werner *et al.* (1976). The accuracy of the fluxes thus obtained is about 30%; the accuracy with which the ratio of two line fluxes is determined is somewhat better than this (15-20%). At 84.5 μm, the different beamsize makes necessary a correction for source coupling, which we estimated on the basis of our [O I] 63.2 μm observations in the direction of BN with both the 30" and 44" beams (see Werner *et al.* 1984 and Ellis and Werner 1985). At this position, the [O I] line is dominated by emission associated with the shocked region. The ratio of [O I] flux in the two beams is 1.5 (44" to 30"), and this factor has been applied to the 30" CO and OH measurements.

The spectrometer's velocity scale was determined by observing fringes of 0.6328 μm He-Ne laser light reflected from the scanning Fabry-Perot interferometer. Wavelength reference points were provided by nearby HDO, $H_2{}^{18}O$ (Kyro 1981, Messer, Helminger and DeLucia 1983), H_2S (Flaud, Camy-Peyret and Johns 1983) and NH_3 lines (Urban *et al.* 1981), which were measured using the spectrometer's internal absorption cell. The CO and OH wavelengths are obtained from measurements by Todd *et al.* (1976) and Brown *et al.* (1982), respectively.

Table 1 is a summary of the observations made with the beam centered on BN. The spectra of the individual CO and OH lines are shown in Figures 1-5. The results

Table 1

CO and OH Lines From Orion-KL

Line	λ (μm)	Flux[a] (10^{-17} W cm^{-2})	Intensity[a,b] (10^{-2} erg s^{-1} cm^{-2} sr^{-1})
CO J = 21→20	124.194	5.1[d]	1.0[d]
OH $^2\Pi_{3/2}$ J = 5/2→3/2	119.441	0.7±0.3	0.15±0.06
	119.234	0.83	0.17
^{13}CO J = 23→22	118.660	<0.3	<0.06
CO J = 22 → 21	118.581	5.3	1.1
CO J = 26 → 25	100.461	1.9	0.38
CO J = 27 → 26	96.7725	3.2(+0.9,-1.9)	0.64(+0.18,-0.38)[d]
OH $^2\Pi_{3/2}$ J = 7/2→5/2	84.5966	0.56[c]	0.17[c]
	84.4202	<0.2[c]	<0.05[c]
CO J = 31 → 30	84.4107	0.6-0.87[c]	0.18-0.26[c]
CO J = 34 → 33	77.0586	0.43	0.086

[a] The uncertainty in the absolute fluxes and intensities is ±30% unless indicated otherwise; the uncertainty in ratios of intensities masured with the same beam is somewhat smaller than this (15-20%).

[b] Averaged over a 44" (FWHM) beam.

[c] 30" beam.

[d] Storey *et al.* (1981).

of the additional OH observations are shown in Figure 6, along with similar "strip maps" in the lines of CO J = 21 → 20 (Storey *et al.* 1981) and H_2 v = 1 → 0 S(1) (R.R.Treffers, personal communication; Beckwith *et al.* 1978). One of the spectra (Figure 2) also covers the J = 23→22 line of ^{13}CO; unfortunately, interference from

telluric O_3 allows only a modest upper limit to be set for the intensity of this line.

The absolute frequency reference for the 84.5 μm observations was obtained by assuming that the longer-wavelength line in Figure 4 is the OH $^2\Pi_{3/2}\, J^p = 7/2^+ \rightarrow 5/2^-$ line, and that its velocity centroid is the same as the 119 μm OH lines. In doing so, we ignore an apparent overall redshift of the spectrum suggested by a calibration with respect to the NH_3 $J = 6 \rightarrow 5$, $s \rightarrow a$ lines produced in the spectrometer's internal gas cell. The apparent redshift would be 24 km s^{-1} (0.4 of a spectral resolution element), and could have been caused by a small misalignment of a mirror. At the spectral resolution of 60 km s^{-1}, the CO $J = 31 \rightarrow 30$ and OH 84.42 μm line are blended. However, the resulting line peaks near the CO wavelength, and the integrated intensity of this feature is not very different from that expected for the CO $J = 31 \rightarrow 30$ line alone on the basis of the intensities of the other CO lines observed. Thus we consider the 84 μm observations to have produced clear detections only of the CO line and the 84.6 μm OH line. We estimate that at least 70% of the intensity of the observed 84.4 μm feature can be accounted for by the CO transition, resulting in a limit on the OH 84.4 μm/84.6 μm ratio of <0.5. (The 84.4 μm feature does seem to show some excess emission on the redshifted side; this may represent the contribution of the OH transition).

At 119.4 μm, the $^2\Pi_{3/2}\, J^p = 5/2^+ \rightarrow 3/2^-$ line is not resolved from the telluric O_3 line at 119.46 μm, and the OH line emission must be corrected for continuum emission absorbed by this line. Another telluric O_3 line at 119.05 μm (see Figure 1), which has 1.9 times the equivalent width of the former O_3 line, provides us with an estimate of this absorption. With the correction, similar intensities for the 119.4 and 119.2 μm OH lines are found.

In addition to the CO and OH data, upper limits to the intensities of the HD $J = 1 \rightarrow 0$ line and several lines in the $J = 5 \rightarrow 4$ and $J = 6 \rightarrow 5$ multiplets of NH_3 were obtained, and are listed in Table 2. The NH_3 data are consistent with the

$J = 4 \rightarrow 3$, $a \rightarrow s$, $K = 3$ detection reported previously (Townes *et al.* 1983), and will not be discussed further here. The HD line was observed at 75 km s^{-1} resolution. Interference from telluric HDO, $H_2^{17}O$ and O_3 lines produced a baseline uncertainty of 2% of the continuum at 112 μm, leading to the upper limit shown in Table 2.

Table 2

HD and NH_3 Upper Limits

Line	λ (μm)	Flux (10^{-17} W cm^{-2})
HD $J = 1 \rightarrow 0$	112.075	<0.1[a]
NH_3 $J = 5 \rightarrow 4$, $a \rightarrow s$, $K = 1$	100.277	<0.5[a]
NH_3 $J = 5 \rightarrow 4$, $a \rightarrow s$, $K = 2$	100.213	<0.5[a]
NH_3 $J = 5 \rightarrow 4$, $a \rightarrow s$, $K = 3$	100.105	<0.5[a]
NH_3 $J = 6 \rightarrow 5$, $a \rightarrow s$, $K = 4$	84.6196	<0.2[b]
NH_3 $J = 6 \rightarrow 5$, $a \rightarrow s$, $K = 5$	84.5422	<0.2[b]

[a] 44" beam.

[b] 30" beam.

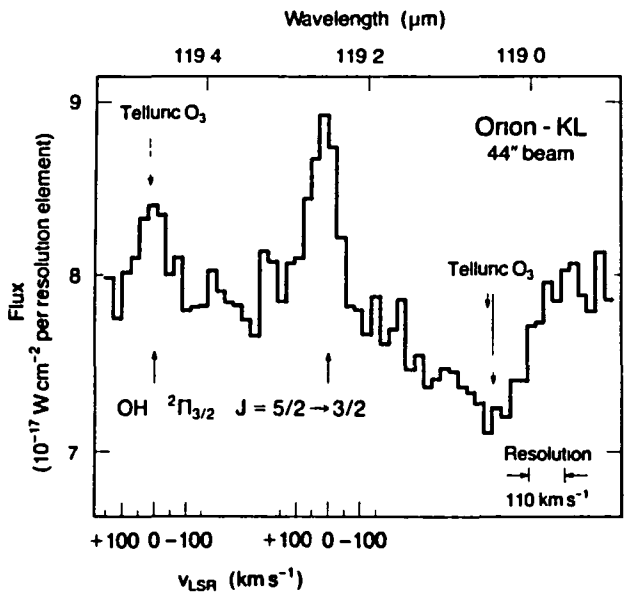

Figure 1: OH $^2\Pi_{3/2}$ J = 5/2 → 3/2 emission in Orion-KL. This spectrum is the result of 7 minutes of integration (6.6 s per point). As discussed in the text, the actual intensities of the two OH lines are very similar after accounting for the effect of the telluric O_3 line at 119.46 μm. The wing of a telluric O_2 line centered at 119.81 μm has been divided out of the spectrum.

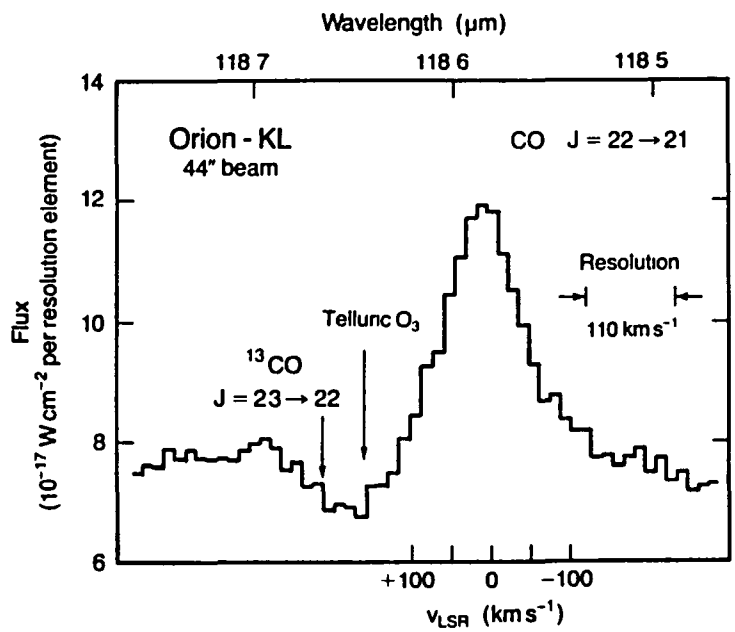

Figure 2: The CO J = 22 → 21 line in Orion-KL. The total integration time for this spectrum was 3 minutes, or 3 s per point. An upper limit to the intensity of the ^{13}CO J = 23→22 line was also derived from this observation.

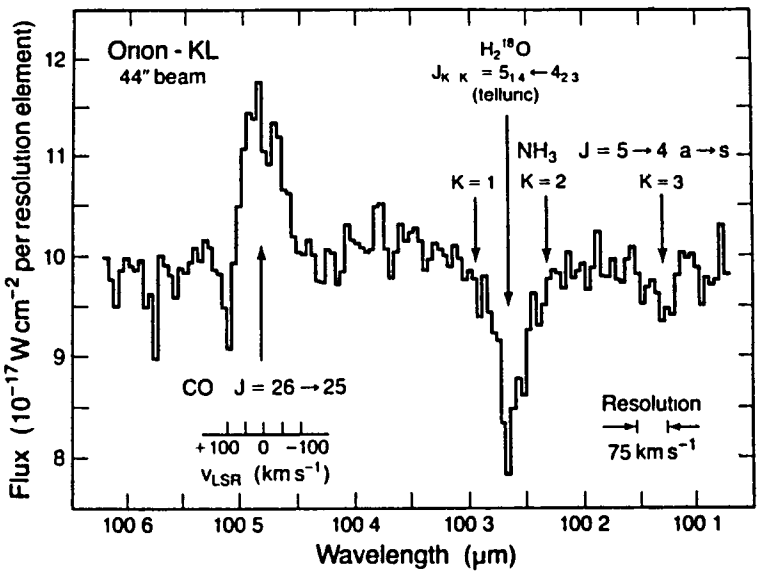

Figure 3: Detection of the CO J = 26 → 25 line in Orion-KL. Note that the line is clearly broader than the unresolved telluric $H_2{}^{18}O$ line. Upper limits to the intensities of three NH_3 lines were also obtained from this spectrum. The total integration time was 30 minutes (14 s per point).

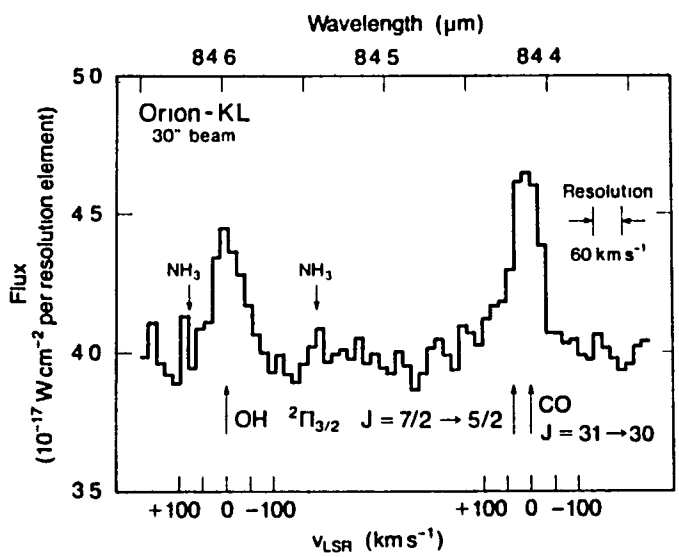

Figure 4: Detection of the OH $^2\Pi_{3/2}$ $J^p = 7/2^- \rightarrow 5/2^+$ and CO J = 31→30 lines in Orion-KL. The velocity scales are appropriate for the CO line and the 84.6 μm OH line, the latter having been taken as the absolute wavelength reference for the observation. At this velocity resolution, the CO line is blended with the OH $^2\Pi_{3/2}$ $J^p = 7/2^+ \rightarrow 5/2^-$ line, but, as discussed in the text, $\gtrsim$70% of the observed line is probably due to the CO transition. Upper limits to the intensities of two NH_3 lines were also obtained from this spectrum. The total integration time was 22 minutes (21 s per point).

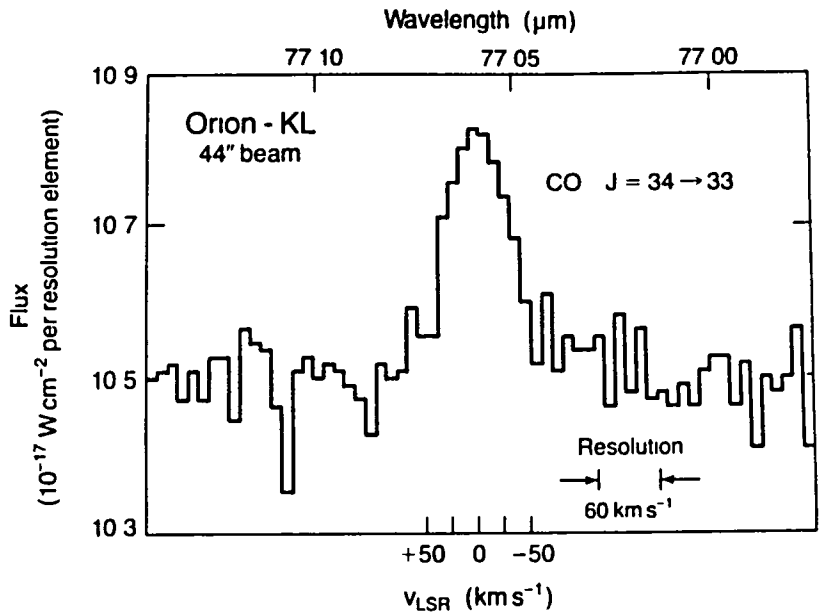

Figure 5: Detection of the CO $J = 34 \rightarrow 33$ line in Orion-KL. The total integration time for this spectrum was 42 minutes (40 s per point). Baseline curvature, caused by strong absorption lines centered on either side of the spectral interval shown above, was removed by dividing by the observed spectrum of Mars.

III. Physical Parameters and Abundance of CO in the Shocked Gas

a) Velocity Distribution

The CO line observations were done at high enough spectral resolution to partially resolve the lines (see Figure 3 in particular). The observed linewidths are all 15-25 km s^{-1} broader than the instrumental full width at half-maximum. This probably indicates that the far-infrared CO lines are narrower than the plateau component of the millimeter-wavelength lines of CO ($\Delta v \approx 50$ km s^{-1}; e.g. Knapp *et al.* 1981) or the H_2 lines at 2 μm ($\Delta v \approx 40$ km s^{-1}; Nadeau, Geballe and Neugebauer 1982, Scoville *et al.* 1982). To show this, we have performed numerical convolutions of these latter lineshapes and our instrumental profile. If the CO plateau profile, observed at very high velocity resolution with beams similar to ours, is taken, the resulting far-infrared CO profile is $\gtrsim 50$ km s^{-1} wider than the instrumental FWHM. In the case of the 2 μm H_2 lines, we take the "intrinsic" H_2 $v = 1 \rightarrow 0$ S(1) profile presented by

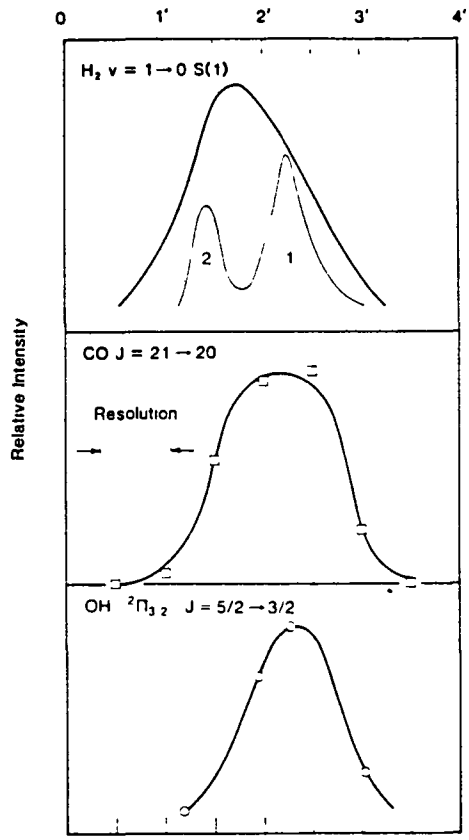

Figure 6: Strip maps of H_2, CO, and OH emission in Orion-KL. The strip lies along a line leading 30 degrees W of N through H_2 Pk 2 (Beckwith *et al.* 1978). The H_2 strips are made with 45" resolution (bold curve) and 13" resolution (thin curve), and come from Treffers (personal communication) and Beckwith *et al.* (1978), respectively. Also shown on the H_2 strip map are the positions of Pk 1 and Pk 2.

Nadeau, Geballe and Neugebauer (1982). This profile results from a weighted average of data from many small-beam measurements covering the bulk of the shocked region, from which the effect of the finite spectrometer resolution (20 km s^{-1}) was removed by numerical deconvolution; it still has the effects of extinction within the shocked region, which makes the observed line narrower than the true velocity

distribution. When convolved with our instrumental profile, the "intrinsic" H_2 profile gives rise to far-infrared CO linewidths which exceed the resolution by 40–50 km s^{-1}, substantially greater than those observed. Since the far-infrared CO lines are not affected by extinction, they would appear still wider than this if they resulted from the same velocity distribution as the 2 μm H_2 lines. Thus the sources of the CO plateau and the 2 μm H_2 lines probably do not contribute much of the observed far-infrared CO emission.

If the far-infrared CO lines have the same shape as the millimeter-wave CO lines, but a different width, the intrinsic width lies in the range 20-30 km s^{-1} (FWHM).

The OH lines are also observed to be about 15-20 km s^{-1} broader than the resolution, and thus may have an intrinsic velocity dispersion similar to that of the far-infrared CO lines.

b) Density, Temperature and CO Abundance

The upper states of the nine far-infrared CO lines observed to date in Orion-KL range in excitation temperature E_J/k from 750 K (J=16) to 3300 K (J=34). Thus the manner in which the shocked gas is sampled by these lines is similar to that for the H_2 v = 0 S(2) line at 12.28 μm, for which E_J/k = 1700 K. In contrast to the H_2 rotational ladder, which is populated according to thermal equilibrium, the far-infrared CO observations involve states which are rather far from thermal equilibrium as well as some which are fairly close, so the CO line ratios are sensitive to density as well as temperature in the shocked gas (Storey *et al.* 1981). Combination of this information and that obtained from observations of the H_2 v = 0 S(2) line yields the CO/H_2 relative abundance and mass of the shocked gas.

The method by which the H_2 density, temperature and CO/H_2 relative abundance are estimated is discussed by Storey *et al.* (1981); we outline it briefly here.

Since the far-infrared CO lines in Orion-KL are unextinguished and optically thin (cf. Watson *et al.* 1980), their intensities are expressed by:

$$I_J = \frac{h\nu}{4\pi} A_J N_J , \qquad (1)$$

where A_J is the A-coefficient for the $J \rightarrow J\text{-}1$ transition and N_J is the column density of CO in the J^{th} state. Given the molecular hydrogen density $n(H_2)$ and temperature T, the N_J's are determined by:

$$N_J \left[A_J + n(H_2) \sum_{J'} \gamma_{JJ'} \right] = N_{J+1} A_{J+1} + n(H_2) \sum_{J'} N_{J'} \gamma_{J'J} , \qquad (2)$$

$$\sum_J N_J = N_{CO} ,$$

where $\gamma_{JJ'}$ is the rate coefficient for the collisional transition $J \rightarrow J'$ and N_{CO} is the total CO column density. It is assumed here that decay of higher vibrational levels pumped by collisions or by radiation in the 4.6 μm CO fundamental vibration bands has a negligible effect on the populations of the rotational levels. This assumption may be made plausible by considering the vibrational collisional excitation rates (Scoville, Krotkov and Wang 1980) and number of available 4.6 μm photons (cf. Downes *et al.* 1981). Values of $n(H_2)$ and T are obtained by finding the solutions to Equations 2 which match the *shape* of the N_J distribution inferred from the observed fluxes. Once $n(H_2)$ and T are known, N_J/N_{CO} is determined for all J, and N_{CO} may be obtained from any of the observed line intensities by using Equation 1. For the molecular constants in Equations 2, we take the collisional rate coefficients $\gamma_{JJ'}$ calculated by S. Green (McKee *et al.* 1982), and compute the A-coefficients using the rigid-rotor approximation and a permanent dipole moment of 0.112 D.[1]

[5] Green and Chapman (1983) and Chackerian and Tipping (1983) have computed higher-order corrections to the collisional rate coefficients and the A-coefficients (respectively). These corrections are not included in the results presented here because they are relatively small and nearly cancelling. Upon repeating our calculations using these corrections, we found the only effect to be a 30% reduction in the derived H_2 density.

Much is already known about the Orion-KL shocked gas from H_2 observations. The latest observations can be summarized as follows. Rotation-vibration transitions at 2 μm and highly-excited pure rotational transitions arise from matter at about 2000 K; this gas lies behind an extinction of 2 magnitudes at 2 μm (Beckwith *et al.* 1983) and its column density, averaged over a 1' diameter area centered on IRS2, is 2.4×10^{19} cm^{-2}. The H_2 v = 0 S(2) line at 12.28 μm has also been observed in this region (Beck, Lacy and Geballe 1979; Beck *et al.* 1982; Beck 1984). A value for the extinction at 12 μm of 0.75 mag can be derived from the 2 μm extinction using standard interstellar extinction curves (Becklin *et al.* 1978). From this, and the observed intensities of the 12.28 μm line, we infer a column density in the v = 0, J = 4 state of 1.5×10^{20} cm^{-2}, averaged over the same 1' diameter area. This obviously cannot be due to the 2000 K gas alone and indicates the presence of an additional amount of somewhat cooler gas. To account for these two batches of gas in the interpretation of the far-infrared CO data, Storey *et al.* (1981) modelled the region with two components, one at 2000 K (designated "hot") and the other one cooler (designated "warm"). The H_2 column densities derived from the 2 μm and 12 μm observations were used along with the solution of Equation 2 and the assumption of pressure equilibrium (so that $n(H_2) \propto 1/T$) to fit the CO relative intensities and thus derive the temperature of the cooler component, the CO/H_2 relative abundance, and the molecular hydrogen density. The present CO observations are more extensive than those available at the time of the earlier calculation, and the accepted value for the average extinction at 2 μm has since changed from 4 mag to 2 mag. Therefore we have repeated the calculation. The range of parameters which produce an acceptable fit is shown in Table 3; the best fit is given by

$$T = 750\ \mathrm{K}$$

$$n(H_2) = 3\times10^{6}\ \mathrm{cm}^{-3}$$

$$N(H_2) = 3\times10^{21}\ \mathrm{cm}^{-2}$$

$$CO/H_2 = 1.2\times10^{-4}$$

for the warm component. The CO intensities resulting from the "best fit" parameters is displayed in Figure 7. Note that the "hot" component, which dominates the 2 μm H_2 emission, contributes very little to the observed far-infrared CO lines, so that ours is essentially a single-component model of the "warm" post-shock gas.

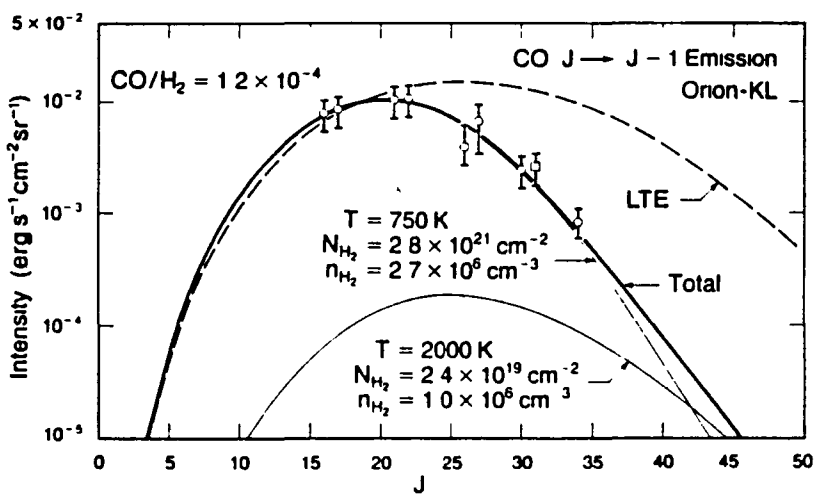

Figure 7: Observed CO line intensities, compared to the simple model discussed in the text. The intensity distribution for T = 750 K, $N(H_2) = 2.8\times10^{21}$ cm^{-2}, and thermal equilibrium (LTE) is also shown. The intensity plotted for the $J = 31\rightarrow30$ line (square symbol) is the full intensity of the 84.4 μm feature, part of which may be due to the nearby OH transition. The 17 → 16 and 16 → 15 points are from Stacey *et al.* (1982, 1983).

Table 3

Two-component Model:

Orion-KL Post-shock Gas

Parameter	"Hot" gas	"Warm" gas
Temperature	2000 K	1000-500 K
$n(H_2)$ (cm^{-3})	$0.5 - 3 \times 10^6$	$1 - 16 \times 10^6$
$N(H_2)$ (cm^{-2})	2.4×10^{19}	$2 - 6 \times 10^{21}$
$M(H_2)$ ($M_\odot$)	0.01	1 - 3
CO/H_2	$1.5 - 0.8 \times 10^{-4}$	$1.5 - 0.8 \times 10^{-4}$

The more important results of the far-infrared CO observations and the simple model described above are the limits placed on the CO/H_2 relative abundance, the H_2 column density and total mass of the post-shock material, and the approximate H_2 density. A single-temperature model for the warm component is of course an oversimplification, since there must be a temperature gradient created by the cooling of the post-shock gas. However, we also note that the derived values of most of the parameters do not change radically over the temperature range where the fit is good, which indicates that similar values would be derived if the source is considered to have temperature variations in this range. The post-shock molecular hydrogen density cannot be much higher than a few times 10^6 cm^{-3}. The CO/H_2 ratio is a more accurate estimate, regardless of the precise values of density and temperature, because it comes from the flux ratio of two lines (CO $J = 22 \rightarrow 21$ and H_2 $v = 0$ S(2)) which are optically thin and arise from states which are nearly thermalized and have similar energies.

IV. Thermal OH Emission from the Shocked Gas

The OH lines reported here are the lowest-lying pure rotational transitions in the $^2\Pi_{3/2}$ electronic state (see Figure 8). The 119 μm OH observations (Figures 1 and 6) confirm the tentative detection by Storey, Watson and Townes (1981). From the strip map of the 119.2 μm line (Figure 6) it appears that the source of the emission is about 1' in size (assuming a Gaussian source) and covers roughly the same region as the far-infrared CO and near-infrared H_2 emission. With the 119.4 μm intensity corrected as discussed above (§ II), no variation of the 119.4/119.2 μm intensity ratio with position is seen. At the position of BN, the intensities of the four OH lines observed are in the proportions 0.9 : 1.0 : 1.0 : <0.5 (119.4 : 119.2 : 84.6 : 84.4 μm).

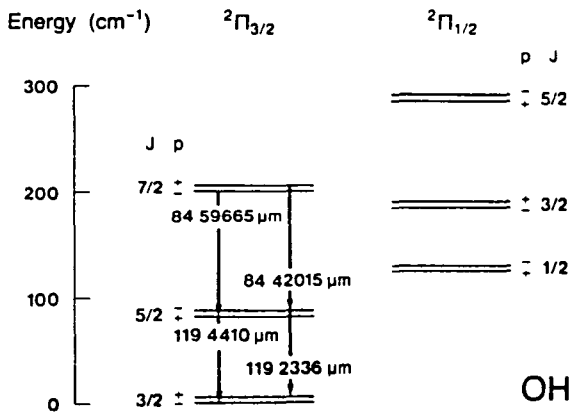

Figure 8: The lowest rotational energy levels of OH, labelled by rotational quantum number J and parity p, showing the observed transitions. The Λ-type splitting is exaggerated in this drawing.

As we will see below, collisional excitation and radiative trapping in the shocked region can reasonably account for the OH emission; purely radiative mechanisms cannot. Both far-infrared and near-infrared pumping can be ruled out by considering the luminosity of the continuum sources and the branching ratios of the

resulting cascades; the continuum at 53 and 37 μm is too weak by at least an order of magnitude to produce the observed lines through a rotational cascade, while the 3 μm continuum sources are at least four orders of magnitude too weak to do so with a vibrational cascade. (Of course, direct rotational pumping by 119 and 84 μm photons cannot work because the OH lines would then appear in absorption rather than emission.) Resonant scattering of far-infrared continuum photons by optically thick OH lines also cannot produce the observed spectra; given the color temperature of dust in the Orion-KL region (80-100 K), resonantly-scattered continuum radiation would produce lines with relative intensities $1 : 1 : \gtrsim 2 : \gtrsim 2$, contrary to observations.

There are considerable uncertainties in the collisional rate coefficients for OH rotational excitation, especially in the relative rates for different Λ-doubling levels with the same angular momentum quantum number J (Andresen *et al.* 1984a,b), so any numerical results derived from the OH intensities must be regarded as very approximate. Nevertheless, it seems clear that the OH relative abundance in Orion-KL is unusually large. The relative abundance of OH may be estimated from the 119 μm line fluxes as follows. Since these lines have rather large A-coefficients (0.138 s^{-1}) and involve the ground rotational state, one might expect them to have large optical depth but small fractional upper-state population. Though the former condition would imply that the photons are absorbed and re-emitted many times on their way out of the cloud, the latter means that collisional de-excitations are not frequent enough to destroy a significant number of them. Thus the line flux should be proportional to the rate of collisional excitations (or, equivalently, the molecular emission measure $\int n_{OH} n(H_2) ds$), just as it would be if the line were optically thin and subthermally excited, though there would be an additional geometry-dependent factor due to the repeated scattering of the line photons. Assuming plane-parallel geometry and the validity of the escape probability approximation, the line intensity I_J is given by (see Appendix A):

$$I_J = \frac{3h\nu}{4\pi} \sum_{J' \geq J} \gamma_{0J'} \, n(H_2) \, N_{OH} \qquad (3)$$

From the observed strength of the pair of 119 μm OH lines, the density of $n(H_2) = 3\times10^6$ cm^{-3} derived in the previous section, and the theoretical collisional excitation rate coefficients at T = 600 K (Dewangan and Flower 1982), we obtain the following values of OH column density and line optical depth averaged over the beam:

$$< N_{OH} > = 1.5\times10^{15} \text{ cm}^{-2} ,$$

$$< \tau > = 3 \quad \text{(each line)} .$$

A line width of 30 km s^{-1} was taken in the calculation of the average optical depth. Both of these average values should be regarded as lower limits to the actual quantities because of the assumption of plane-parallel geometry and since the source is not likely to uniformly fill the beam. As may be easily shown, these results imply small excited-state populations as long as the beam filling factor is larger than about 0.05.

The OH emission appears somewhat more localized around Pk 1 than does the CO; the two may not be identically distributed. However, if the distributions are taken to be approximately the same, a relative OH abundance of $OH/H_2 = 5 \times 10^{-7}$ is implied. Because of the assumptions of plane-parallel geometry and distribution throughout the shocked layer, this is a *lower* limit to the local OH/H_2 ratio, yet it is more than an order of magnitude greater than the OH/H_2 ratio under any conditions which are likely to be found in dense, quiescent molecular clouds (Prasad and Huntress 1980). Such an overabundance is the expected outcome of the elevated temperature in a post-shock molecular environment, in which endothermic or high-threshold reactions between neutral molecules can occur; in particular, the reaction $O + H_2 \rightarrow OH + H$ (Hollenbach and McKee 1979, 1980).

V. Limits on the D/H Ratio in OMC-1

The line-to-continuum ratio of the $J = 1 \rightarrow 0$ transition of HD can be used to obtain the HD/H_2 abundance ratio (= 2D/H) in dense molecular clouds such as Orion. Because HD is expected to bear most of the deuterium in molecular clouds, this measurement of D/H is free of the effects of chemical isotopic fractionation which introduce uncertainties in D/H determinations by millimeter-wavelength lines of trace species. Since the $J = 1$ state is only 128 K above ground, emission from the direction of Orion-KL would be dominated by the warm, quiescent core of OMC-1, for which $T_{gas} \sim T_{dust} \sim 70$ K, $N(H_2) \sim 10^{24}$ cm^{-2} and $\tau_D \sim 0.3$ for the 100 μm continuum emission from the central 1' (cf. Werner 1982). In Appendix B, the following expression is derived for the HD/H_2 ratio in such clouds:

$$\frac{HD}{H_2} = \left(\frac{\Delta\nu_C}{\nu}\right)\left(\frac{T}{13\,K} + 1.7 + \frac{22\,K}{T}\right)\left(\frac{1}{1 - e^{-128.4\,K/T}}\right)\left(\frac{e^{\tau_D} - 1}{\tau_D}\right)\left(\frac{I(1\rightarrow 0)}{I_C}\right) , \qquad (4)$$

where $\Delta\nu_C/\nu$ is the effective fractional continuum bandwidth of the spectrometer ($\pi\Delta\nu_{FWHM}/2\nu$ for a Fabry-Perot interferometer) and $I(1\rightarrow 0)$ is the integrated intensity of the line. With the above values of temperature and continuum optical depth, the upper limit of 0.02 for the line-to-continuum ratio implies $HD/H_2 < 8\times10^{-5}$, or:

$$\frac{D}{H} < 4\times10^{-5} .$$

The interstellar abundance of deuterium, which is thought to be near 10^{-5}, is not very strongly constrained by this measurement.

VI. Comparison with Theoretical Models

Although the density and temperature estimates obtained from the far-infrared CO observations are not very precise, they are good enough to rule out the possibility that a purely hydrodynamic (non-dissociative non-magnetic, or NDNM) shock is responsible for the H_2 and CO emission in Orion-KL, as may be seen quite simply. Such a shock would have an initial compression of a factor of 6, with an accompanying temperature jump from T_0 to T_{max}. The post-shock gas would have approximately constant pressure, so that the post-shock density would be $n = 6\, n_0\, T_{max}/T$. Near-infrared observations of H_2 lines (e.g. Beckwith *et al.* 1983, Beck and Beckwith 1983) and conservation of energy provide constraints on the maximum temperature and preshock density:

$$T_{max} \sim 2700\ \mathrm{K}\,,$$

$$n_0 \gtrsim 4\pi I(H_2)/\,m(H_2)\, v_s^3 \gtrsim 10^6 \mathrm{cm}^{-3}\,,$$

since the shock speed v_s must be $\lesssim 15$ km s^{-1} to keep the molecular hydrogen from being collisionally dissociated (cf. Kwan 1977). By the time the post-shock gas would have cooled to 750 K, the density would have been $\gtrsim 2\times10^7$ cm^{-3}, and thus all of the states from which the far-infrared CO lines originate would be thermalized at high temperature, in conflict with the observations.

Because of this difficulty with NDNM shock models, and the additional problem posed by the very large velocity widths seen in the near-infrared H_2 lines (Nadeau, Geballe, and Neugebauer 1982, Scoville *et al.* 1982), theoretical attention has turned to hydromagnetic shocks (Draine 1980, Draine, Roberge and Dalgarno 1983, McKee, Chernoff and Hollenbach 1984, Draine and Roberge 1984). These shock structures have been applied specifically to Orion-KL by Chernoff, Hollenbach and

Table 4

Comparison of Models and Observations

Line	Wavelength (μm)	Observed intensity (10^{-2} erg s^{-1} cm^{-2} sr^{-1})	Calculated intensity[b] (10^{-2} erg s^{-1} cm^{-2} sr^{-1})	
			CHM	DR
CO	124.2	1.0[a]	0.90	0.98
OH	119.4	0.15	0.18	0.17
OH	119.2	0.17	0.18	0.17
CO	118.6	1.1	...	0.92
CO	100.5	0.38	...	0.56
CO	96.77	0.64[a]	0.40	0.55
CO	87.19	0.24[a]	0.22	0.22
OH	84.60	0.17	0.22	...
OH	84.42	<0.08	0.22	...
CO	84.41	0.18-0.26	...	0.15
CO	77.06	0.086	0.10	0.068

[a] Storey *et al.* (1981).
[b] CHM ≡ Chernoff, Hollenbach and McKee (1982); DR ≡ Draine and Roberge (1982).

McKee (1982) and Draine and Roberge (1982). Calculated line intensities from these models are compared with the present far-infrared observations in Table 4, and the model parameters are listed in Table 5. In both cases, close agreement with experiment is obtained with "C-type" shocks (no discontinuous "jumps" in the fluid parameters).

Table 5

Model Parameters

Parameter	CHM	DR
$n_0(H_2)$ (cm $^{-3}$)	1×10^5	3.5×10^5
$A_{2\mu m}$ (mag)	2.5	4[a]
$A_{12\mu m}$ (mag)	0.94	0.8[a]
v_s (km s^{-1})	36	38
CO/H_2	6×10^{-4}	1.4×10^{-4}[a]
B_0 (mG)	0.45	1.5

[a]Assumed in all model calculations. Other values result from free-parameter fits.

VII. Summary

The more important results of the far-infrared molecular line observations of Orion-KL are the following.

1. Downstream from the 2000 K shocked gas seen in the 2 μm H_2 lines, there is a much larger, cooler component of post-shock gas with column density $N(H_2) \approx 3 \times 10^{21}$ cm^{-2}, total mass $M \approx 1$ $M_\odot$ and characteristic temperature and density $T \approx 750$ K and $n(H_2) \approx 3 \times 10^6$ cm^{-3}. The density is too low by at least an order of magnitude for the shock to be non-dissociative and non-magnetic.

2. The far-infrared CO and OH lines arising in this shocked gas have velocity dispersions of $\Delta v \approx 20$-30 km s^{-1} (FWHM), somewhat less than either the 2 μm H_2 lines or the high-velocity plateau component of the millimeter-wave CO lines. The far-infrared CO lines are optically thin; the 119 μm OH lines have $\tau \gtrsim 3$.

3. The relative abundance of CO is $CO/H_2 \approx 1.2 \times 10^{-4}$, corresponding to about 20% of the cosmic abundance of C tied up in CO. Since no significant creation or destruction of CO is expected to take place in the shock, this probably represents the normal CO relative abundance in the Orion cloud, and can be compared with the value of $\gtrsim 12\%$ determined by Dickman (1978) from a ^{13}CO dark-cloud survey.

4. The average relative abundance of OH in the warm postshock gas is $OH/H_2 \gtrsim 5\times10^{-7}$, more than an order of magnitude greater than that expected in the quiescent pre-shock gas.

5. The relative abundance of deuterium in the core of the Orion molecular cloud is $D/H < 4\times10^{-5}$.

We wish to thank the staff of the Kuiper Airborne Observatory for their excellent support of this experiment. We are also grateful to S.C. Beck, D.F. Chernoff, B.T. Draine, D.R. Flower, S. Green, D.J. Hollenbach, C.F. McKee, E. Serabyn and R.R. Treffers for discussing their results with us, and to M.K. Crawford for assistance with the observations. This project was supported in part by NASA grant NGR 05-003-511.

Appendix A

Derivation of Equation 3

Let us assume the validity of the escape probability approximation and consider the transition $k \rightarrow j$ in a molecule for which the absorption coefficient of the line is much greater than that of the dust. (This includes the lower rotational transitions of the most common molecules except those of molecules with zero or extremely

small dipole moments, like H_2 or HD). The intensity I_{kj} emitted in this line, in excess of the continuum, is given by

$$I_{kj} = \int d\nu\, \varphi(\nu) \left[S_{kj}\,(1-\beta_{kj}) - B_\nu(T_D)\,(1-e^{-\tau_D}) \right] , \qquad \text{(A1)}$$

where $\varphi(\nu)$ is the line profile and S_{kj} and β_{kj} are the source function and escape probability for the line. We can neglect the term due to dust emission and absorption, since in the present application (shocked gas), the dust optical depth τ_D is small and the dust temperature T_D is much lower than the gas temperature. In the limit of small population in the upper state k, the source function is simply

$$S_{kj} \cong \frac{2h\nu^3}{c^2} \; \frac{n_k}{n_j} \; \frac{g_j}{g_k} , \qquad \text{(A2)}$$

where the g's are the degeneracies of the given states. In the same limit, with state j as the ground state, the equations of statistical equilibrium which determine the population of state k reduce to

$$n_j\, n(H_2) \sum_{i \geq k} \gamma_{ji} = n_k\, n(H_2)\, \gamma_{kj} + n_k\, \beta_{kj}\, A_{kj} , \qquad \text{(A3)}$$

Under the assumption that the effective radiation rate $\beta_{kj}\, A_{kj}$ is much larger than the collisional de-excitation rate $n(H_2)\, \gamma_{kj}$, we obtain

$$I_{kj} \cong \int d\nu\, \varphi(\nu)\, \frac{2h\nu^3}{c^2} \; \frac{g_j}{g_k} \; \frac{\sum_{i \geq k} n(H_2)\, \gamma_{ji}}{\beta_{kj}\, A_{kj}} \qquad \text{(A4)}$$

In a plane-parallel cloud with a large velocity gradient, the escape probability is as given by Scoville and Solomon (1974):

$$\beta_{kj} = \frac{1 - e^{-3\tau_{jk}}}{3\tau_{jk}} \approx \frac{1}{3\tau_{jk}} , \qquad \text{(A5)}$$

where the optical depth τ_{jk} (assumed large) is given by

$$\int d\nu\, \varphi(\nu)\, \tau_{jk} = \frac{h\nu}{c}\,(N_j\, B_{jk} - N_k\, B_{kj})$$

$$\approx \frac{h\nu}{c}\, N_j\, B_{jk} \qquad \text{(A6)}$$

$$\approx \frac{c^2}{8\pi\nu^2}\,\frac{g_k}{g_j}\, A_{kj}\, N_j$$

(Note that under the approximations we have made so far, $N_{\text{total}} \approx N_j$). Finally, taking the line profile $\varphi(\nu)$ to be narrow, we obtain

$$I_{kj} = \frac{3h\nu}{4\pi} \sum_{l \geq k} \gamma_{jl}\, n(H_2)\, N_j\ . \qquad \text{(A7)}$$

This expression is identical to Equation 3, which is used above to compute the OH column density from the ground-state rotational lines at 119 μm.

Appendix B

Derivation of Equation 4

The HD molecule has a very small permanent dipole moment ($\mu = 5.9\times10^{-4}$ D; Trefler and Gush 1968). Thus its rotational energy levels reach thermal equilibrium at very low densities, and its rotational lines are optically thin. In fact, the transfer of HD line radiation in molecular clouds is controlled by dust absorption, since even for very narrow lines the HD line absorption coefficient, given by

$$\kappa_{J\leftarrow J-1} = \frac{8\pi^3 \mu^2_{J-1,J}}{3hc}\,\frac{\nu}{\Delta\nu}\,\frac{g_J}{g_{J-1}}\, n_{J-1}\left(1 - e^{-h\nu/kT}\right)\ , \qquad \text{(B1)}$$

is much smaller than that of interstellar dust, for which

$$\kappa_D \approx 10^{-24}\left[\frac{n(H_2)}{1\ \text{cm}^{-3}}\right]\left[\frac{125\ \mu\text{m}}{\lambda}\right] \qquad \text{(B2)}$$

(Savage and Mathis 1979, Whitcomb *et al.* 1981). Giant molecular clouds often have substantial far-infrared continuum optical depth, and this must be accounted for in the interpretation of HD intensities. Here, we will once again assume the validity of the escape probability formalism, and compute the HD $J = 1 \rightarrow 0$ line intensity. Consider a dense, quiescent cloud in which the gas and dust are in thermal equilibrium, so that the source function S_ν is equal to the same Planck function for the HD line and the dust continuum. The escape probability for continuum photons is approximately $\beta_D = e^{-\tau_D}$, where $\tau_D = -\int \kappa_D ds$ is the continuum optical depth, and the escape probability for line photons can be written as $\beta_L \beta_D$, where β_L is the probability for a photon to escape line absorption. Since the self-absorption of HD is very small, we take $\beta_L = 1 - \tau_L$, where $\tau_L = -\int \kappa_{1\leftarrow 0} ds$ is the portion of the total optical depth due to the line. Then the excess of specific line intensity above the continuum can be written as

$$\Delta I_\nu = B_\nu(T)\left[1 - \beta_L \beta_D\right] - B_\nu(T)\left[1 - \beta_D\right]$$

$$= \tau_L B_\nu(T) e^{-\tau_D} \quad . \tag{B3}$$

The present measurements would not spectrally resolve lines originating in quiescent clouds, so we compute the integrated line intensity $I(1 \rightarrow 0)$:

$$I(1 \rightarrow 0) = \int d\nu \varphi(\nu) \Delta I_\nu = e^{-\tau_D} \int d\nu \int ds\, B_\nu \kappa_{1\leftarrow 0}$$

$$= e^{-\tau_D} \int d\nu \int ds\, j_{1\rightarrow 0} \quad \text{(in LTE)}$$

$$= \frac{h\nu}{4\pi} A_{1\rightarrow 0} f_1 N_{HD} e^{-\tau_D} \quad . \tag{B4}$$

In thermal equilibrium, the fractional population of the $J = 1$ rotational state is adequately approximated by

$$f_1 = \frac{3e^{-h\nu/kT}}{\frac{2kT}{h\nu} + \frac{1}{3} + \frac{h\nu}{30kT}} \qquad \text{(B5)}$$

The intensity of dust continuum adjacent to the line is given by

$$I_C = B_\nu(T)\left(1 - e^{-\tau_D}\right)\Delta\nu_C \ , \qquad \text{(B6)}$$

where $\Delta\nu_C$ is the continuum bandwidth of the spectrometer. By combining Equations B2, B4, B5 and B6, we obtain

$$\frac{HD}{H_2} = \left(\frac{\Delta\nu_C}{\nu}\right)\left(\frac{T}{13\ K} + 1.7 + \frac{22\ K}{T}\right)\left(\frac{1}{1 - e^{-128.4\ K/T}}\right)\left(\frac{e^{\tau_D} - 1}{\tau_D}\right)\left(\frac{I(1\rightarrow 0)}{I_C}\right) \ . \qquad \text{(B7)}$$

This expression is used above (section V) to derive an upper limit for the D/H relative abundance in core of OMC-1.

References

Andresen, P., Ondrey, G.S., Titze, B. and Rothe, E.W. 1984a, *J. Chem. Phys.* **80**, 2548.

Andresen, P., Hausler, D. and Lulf, H.W. 1984b, *J. Chem. Phys.* **81**, 571.

Bally, J. and Lada, C.J. 1983, *Ap. J.* **265**, 824.

Beck, S.C. 1984, *Ap. J.* **281**, 205.

Beck, S. C., and Beckwith, S. 1983, *Ap. J.* **271**, 175.

Beck, S. C., Bloemhof, E. E., Serabyn, E., Townes, C. H., Tokunaga, A. T., Lacy, J. H., and Smith, H. A., 1982, *Ap. J.* (*Letters*) **253**, L83.

Beck, S. C., Lacy, J. H. and Geballe, T. R. 1979, *Ap. J.* (*Letters*) **234**, L213.

Becklin, E. E., Matthews, K., Neugebauer, G., and Willner, S., 1978, *Ap. J.* **220**, 831.

Beckwith, S., Evans, N. J. II, Gatley, I., Gull, G., and Russell, R. W., 1983, *Ap. J.* **264**, 152.

Beckwith, S., Persson, S. E., Neugebauer, G., and Becklin, E. E., 1978, *Ap. J.* **223**, 464.

Brown, J. M., Schubert, J. E., Evenson, K. M., and Radford, H. E., 1982, *Ap. J.* **258**, 899.

Chackerian, C. and Tipping, R.H. 1983, *J. Mol. Spec.* **99**, 431.

Chernoff, D.F., Hollenbach, D.J. and McKee, C.F., 1982, *Ap. J.* (*Letters*) **259**, L97.

Cudworth, K. M., and Herbig, G. 1979, *Astron. J.* **84**, 548.

Dewangan, D. P., and Flower, D. R. 1982, *M.N.R.A.S.* **199**, 457.

Dickman, R. L., 1978, *Ap. J.* (*Supplement*) **37**, 407.

Downes, D., Genzel, R., Becklin, E. E., and Wynn-Williams, C. G., 1981, *Ap. J.* **244**, 869.

Draine, B.T. 1980, *Ap. J.* **241**, 1021.

Draine, B.T., Roberge, W.R. and Dalgarno, A. 1983, *Ap. J.* **264**, 485.

Draine, B.T. and Roberge, W.R. 1982, *Ap. J. (Letters)* **259**, L92.

_____. 1984, *Ap. J.* **282**, 491.

Ellis, H.B. and Werner, M.W. 1985, in preparation.

Flaud, J.M., Camy-Peyret, C. and Johns, J.W.C. 1983, *Can. J. Phys.* **61, 1462.**

Gautier, T. N. III, Fink, U., Treffers, R. R., and Larson, H. P., 1976, *Ap. J. (Letters)* **207**, L129.

Genzel, R., and Downes, D., 1977, *Astron. Ap. (Supplement)* **30**, 45.

Genzel, R., Reid, M. J., Moran, J. M., and Downes, D., 1981, *Ap. J.* **244**, 884.

Green, S., and Chapman, S., 1983, *Chem. Phys. Lett.* **98**, 467.

Hollenbach, D. J., and McKee, C. F., 1979, *Ap. J. (Supplement)* **41**, 555.

Hollenbach, D. J., and McKee, C. F., 1980, *Ap. J. (Letters)* **241**, L47.

Knapp, G. R., Phillips, T. G., Huggins, P. J., and Redman, R. O., 1981, *Ap. J.* **250**, 175.

Knowles, S.H., Mayer, C.H., Cheung, A.C., Rank, D.M. and Townes, C.H. 1969, *Science* **163**, 1055.

Kwan, J., 1977, *Ap. J.* **216**, 713.

Kyro, E., 1981, *J. Mol. Spec.* **88**, 167.

McKee, C.F., Chernoff, D.F. and Hollenbach, D.J. 1984. In *Galactic and Extragalactic Infrared Spectroscopy (ESLAB Symposium XVI)*, ed. M.F. Kessler and J.P. Phillips (Dordrecht: Reidel), 103.

McKee, C. F., Storey, J. W. V., Watson, D. M., and Green, S., 1982, *Ap. J.* **259**, 647.

Messer, J.K., Helminger, P. and DeLucia, F.C. 1983 *Int. J. IR and mm Waves* **4**, 505.

Nadeau, D., Geballe, T. R., and Neugebauer, G., 1982, *Ap. J.* **253**, 154.

Prasad, S.S. and Huntress, W.T. 1980, *Ap. J.* (*Supplement*) **43**,1.

Savage, B.D. and Mathis, J.S. 1979, *Ann. Rev. Astron. Astrophys.* **17**, 73.

Scoville, N.Z., Hall, D.N.B., Kleinmann, S.G. and Ridgway, S.T. 1982, *Ap. J.* **253**, 136.

Scoville, N. Z., Krotkov, R., and Wang, D., 1980, *Ap. J.* **240**, 929.

Scoville, N.Z. and Solomon, P.M. 1974, *Ap. J.* (*Letters*) **187**, L67.

Snell, R. L., Loren, R. B., and Plambeck, R. L., 1980, *Ap. J.* (*Letters*) **239**, L17.

Stacey, G.J., Kurtz, N.T., Smyers, S.D., Harwit, M., Russell, R.W. and Melnick, G. 1982, *Ap. J.* (*Letters*) **257**, L37.

Stacey, G.J., Kurtz, N.T., Smyers, S.D. and Harwit, M. 1983, *M.N.R.A.S.* **202**, 25p.

Storey, J. W. V., Watson, D. M., and Townes, C. H., 1980, *Int. J. IR* and *mm Waves* **1**, 15.

Storey, J.W.V., Watson, D.M. and Townes, C.H. 1981, *Ap. J.* (*Letters*) **244**, L27.

Storey, J. W. V., Watson, D. M., Townes, C. H., Haller, E. E., and Hansen, W. L., 1981, *Ap. J.* **247**, 136.

Strelnitskii, V. S., and Syunyaev, R. A., 1973, *Sov. Astron.* **16**, 579.

Todd, T. R., Clayton, C. M., Telfair, W. B., McCubbin, T. K. Jr., and Pliva, J., 1976, *J. Mol. Spec.* **62**, 201.

Townes, C.H., Genzel, R., Watson, D.M. and Storey, J.W.V. 1983, *Ap. J.* (*Letters*) **269**, L11.

Trefler, M. and Gush, H.P. 1968, *Phys. Rev. Lett.* **20**, 703.

Urban, S., Spirko, V., Papousek, D., Kauppinen, J., Belov, S.P., Gershtein, L.I. and Krupnov, A.F. 1981, *J. Mol. Spec.* **88**, 274.

Watson, D. M., Storey, J. W. V., Townes, C. H., Haller, E. E., and Hansen, W. L., 1980, *Ap. J.* (*Letters*) **239**, L129.

Watson, D. M., 1982, Ph.D. thesis, University of California, Berkeley.

Werner, M.W., Gatley, I., Harper, D.A., Becklin, E.E., Loewenstein, R.F., Telesco, C.M. and Thronson, H.A. 1976, *Ap. J.* **204**, 420.

Werner, M.W. 1982, *Proceedings of the Symposium on the Orion Nebula To Honor Henry Draper*, ed. Glassgold, A.E., Huggins, P.J. and Shucking, E.L.; *Ann. N.Y. Acad. Sci.* **395**, 79.

Werner, M.W., Crawford, M.K., Genzel, R., Hollenbach, D.J., Townes, C.H. and Watson, D.M. 1984, *Ap. J.* (*Letters*) **282**, L81.

Whitcomb, S.E., Gatley, I., Hildebrand, R.H., Keene, J., Sellgren, K. and Werner, M.W. 1981, *Ap. J.* **246**, 416.

Zuckerman, B., Kuiper, T. B. H., and Rodriguez-Kuiper, E. N., 1976, *Ap. J.* (*Letters*) **209**, L137.

Authors' Addresses

R. Genzel and C. H. Townes: Department of Physics, University of California, Berkeley, CA 94720.

J. W. V. Storey: School of Physics, University of New South Wales, P. O. Box 1, Kensington, NSW 2033, Australia.

Dan M. Watson: Downs Laboratory of Physics, 320-47, California Institute of Technology, Pasadena, CA 91125.

1 Report No	2 Government Accession No	3 Recipient's Catalog No
NASA TM-86721		

4 Title and Subtitle	5 Report Date
FAR-INFRARED EMISSION LINES OF CO AND OH IN THE ORION-KL MOLECULAR SHOCK	September 1985
	6 Performing Organization Code

7 Author(s)	8 Performing Organization Report No
Dan M. Watson,*† R. Genzel,* C. H. Townes,* and J. W. V. Storey‡§	85222
	10 Work Unit No
9 Performing Organization Name and Address	
*University of California, Berkeley, CA 94720, †California Institute of Technology, Pasadena, CA 91125, ‡Anglo-Australian Observatory, P.O. Box 296, Epping, New South Wales 2121, Australia, §University of New South Wales, P.O. Box 1, Kensington, NSW 2033, Australia	11 Contract or Grant No
	13 Type of Report and Period Covered
12 Sponsoring Agency Name and Address	Technical Memorandum
National Aeronautics and Space Administration Washington, DC 20546	14 Sponsoring Agency Code 352-02-03

15 Supplementary Notes

Preprint Series #30. Supported by NASA grants.

Point of Contact. L. C. Haughney, Ames Research Center, M/S 211-12, Moffett Field, CA 94035
(415)694-5339 or FTS 464-5339

16 Abstract

Observations of far-infrared rotational emission lines which arise in the shocked gas associated with Orion-KL are presented, including detections of the CO $J = 34 \rightarrow 33$, $J = 31 \rightarrow 30$, $J = 26 \rightarrow 25$, and $OH^2\Pi_{3/2}\, J^P = 7/2^- \rightarrow 5/2^+$ emission lines, as well as improved measurements of the CO $J = 22 \rightarrow 21$ and $OH^2\Pi_{3/2}$ $J = 5/2 \rightarrow 3/2$ lines. These lines are observed to have velocity widths of $\Delta v \sim 20$-30 km s^{-1}, somewhat less than either the 2 μm H_2 lines or the high-velocity "plateau" component of the millimeter-wave CO lines seen in this object. An H_2 column density of $\sim 3 \times 10^{21}$ cm^{-2}, a total mass of $\sim 1\ M_\odot$ and characteristic temperature and density $T \sim 750$ K and $\sim 2 \times 10^6$ cm^{-3} can be derived from the CO intensities. The density is too low by at least an order of magnitude for the observed infrared H_2 and far-infrared CO emission to be accounted for by a purely hydrodynamic shock, and support is lent to hydromagnetic shock models.

From the present measurements, the relative abundance of CO is estimated to be $CO/H_2 \approx 1.2 \times 10^{-4}$, corresponding to 20% of the cosmic abundance of C existing in the form of CO. The average relative abundance of OH in the shocked gas is $OH/H_2 \gtrsim 5 \times 10^{-7}$, more than an order of magnitude greater than that expected in the quiescent molecular material surrounding the shocked region. The CO lines are optically thin, and the OH lines have $\tau \gtrsim 3$. An upper limit to the intensity of the HD $J = 1 \rightarrow 0$ line is used to derive an upper limit of 4×10^{-5} for the D/H relative abundance in the Orion cloud core.

17 Key Words (Suggested by Author(s))	18 Distribution Statement
Far-infrared: CO and OH spectra Interstellar: Shocked gasses Nebulae: Orion K-L	Unlimited Subject Category - 89

19 Security Classif (of this report)	20 Security Classif (of this page)	21 No of Pages	22 Price*
Unclassified	Unclassified	35	A04

*For sale by the National Technical Information Service, Springfield, Virginia 22161

End of Document